KU LEUVEN

Citation	. C. Clasen **A Self-Aligning Parallel Plate (SAPP) fixture for tribology and high shear rheometry** Rheologica Acta 52 (2013), 191-200.
Archived version	Author manuscript: the content is identical to the content of the published paper, but without the final typesetting by the publisher
Published version	*The final publication is available at Springer via* http://dx.doi.org/10.1007/s00397-013-0683-9
Journal homepage	http://link.springer.com/journal/397
Author contact	your email christian.clasen@cit.kuleuven.be
IR	url in Lirias https://lirias.kuleuven.be/handle/123456789/363250

(article begins on next page)

Special issue devoted to novel trends in rheology

A Self-Aligning Parallel Plate (SAPP) fixture for tribology and high shear rheometry

Christian Clasen

Department of Chemical Engineering,

University of Leuven (KU Leuven),

Willem de Croylaan 46, 3001 Heverlee, Belgium

Abstract

This paper introduces a novel self-aligning parallel plate fixture (SAPP) for rotational rheometers. The ring-shaped shearing surface of this fixture is held on a low friction single contact point bearing and uses hydrodynamic lubrication forces in order to maintain the parallelism of the freely tilting surfaces over a full rotation. The optimized parallelism of the plates enables to conduct tribological measurements of low frictional stress between the shearing surface materials and a fluid at normal loads down to 1.3 kPa. Limited only by the degree of non-flatness of the surfaces, the new fixture can determine boundary lubrication sliding frictions within 10% and down to angular velocities of 400 µrad/s. In a controlled gap mode this setup reaches a gap error of 3.4 µm which enables to reliably conduct rheological measurements down to absolute gaps of the parallel plates of 10 µm and to reach high shear rates up to 10^5 s^{-1}.

Introduction

The determination of viscoelastic properties at high shear rates has always been a challenge, but is at the same time of importance as many processes involve deformation rates that reach easily orders of 10^5 s^{-1}, as in for example coating or lubrication flows, spraying and atomization, extrusion or injection molding (Tadmor and Gogos 2006). One strategy to achieve and measure such high shear rates $\dot{\gamma}$ involves high shearing surface velocities (Mriziq, Dai et al. 2004; Mriziq, Cochran et al. 2007) or high flow rates in capillary or microchannel rheometers (Duda, Klaus et al. 1988; Erickson, Lu et al. 2002; Kang, Lee et al. 2005), also with an *in situ* determination of the pressure drop in the channel as demonstrated by Chevalier et al. (Chevalier and Ayela 2008) and recently by Pipe et al. (Pipe, Majmudar et al. 2008).

A second strategy aims at reducing the gap distance over which the velocity is applied in order to increase $\dot{\gamma}$. Such designs include small gap Searl type geometries, operating at constant gaps down to 1 μm (Merrill 1954), small angled cup/bob devices that allow systematic variation of a small, relative gap (Barnes 2002), and (similar to the case present in this paper) rotary parallel plate rheometers operating at micrometer gaps (Kulicke and Porter 1980; Connelly and Greener 1985; Kramer, Uhl et al. 1987; Henson and Mackay 1995; Dontula, Macosko et al. 1999; Mriziq, Dai et al. 2004; Davies and Stokes 2008; Pipe, Majmudar et al. 2008). Clasen et al. (Clasen and McKinley 2004; Clasen, Gearing et al. 2006; Kojic, Bico et al. 2006; Baik, Moldenaers et al. 2011; Erni, Varagnat et al. 2011; Clasen 2012) introduced with the flexure-based microgap rheometer (FMR) a sliding plate configuration that can set and maintain absolute gaps in the range of 1 - 100 μm and with which shear rates up to 10^5 s^{-1} could be realized (Baik, Moldenaers et al. 2008; Clasen, Kavehpour et al. 2010).

Recent approaches to study tribology and high shear rheology in thin films have looked again at commercially available rotational rheometers and their capability to use their parallel plate fixtures at small gap separations. The possibility to easily determine an absolute zero position and to set with micrometer precision a desired gap between the shearing surfaces has spawned a number of publications that probe the applicability of parallel plate fixtures for high shear rate rheometry (Pipe, Majmudar et al. 2008; Kelly, Gough et al. 2009; Crawford, Williams et al. 2012).

The main problems that arise when setting such small apparent gaps are from misalignment of the shearing surfaces towards each other (parallelism), the surface alignment towards the rotational axis of the rheometer (perpendicularity) and a possible bending or torsion of the surface itself (flatness) (it should be noted that the use of the terms parallelism and flatness in rheological literature is ambiguous and also used with regard to the alignment of the rotational axes). Regularly these errors are combined into a total gap error ε with which the apparent gap is corrected in order to determine the actually effective shear rate applied to a sample. This gap error is usually determined from an extrapolation of measurements with a calibration oil at different gap settings. Still, since the gap error is not arising from an imprecisely set gap, but rather from misalignments of the surfaces, the method of correcting the apparent gap with the determined error can no longer be used when the gap settings h approach the order of magnitude of the error ε. At this point the misalignment is directly affecting the flow field and thus the measured torque, and prohibits therefore a qualitative evaluation of the data below this limit.

Exploring this lower gap limit, Mackay and coworkers showed that it is possible (with a very well-aligned rotational rheometer and specially-machined parallel plates) to perform steady shear experiments down to gaps of $h = 10$ µm (Henson and Mackay 1995). Stokes and co-workers recently presented a study (Davies and Stokes 2008) in which they evaluated the capability of commercially available rotary rheometers for accessing shearing gaps below 100 µm with parallel plates that were, however, selected from a number of similar fixtures with regard to their perpendicularity error. With this they were able to achieve total gap errors as low as $\varepsilon = 25$ µm.

Similar to the problems of setting a precise gap, misalignment of the plates has also limited the use of parallel plate fixtures in a tribological mode for the determination of a sliding friction between the shearing surfaces mediated by a lubricating liquid under an applied normal load. The aim of such tribological measurements is to determine in the 'boundary lubrication' regime at low sliding velocities the friction coefficient between the shearing surfaces. Following Coulomb's friction laws the coefficient is in this velocity regime constant for a surface material/fluid type combination, and independent of the fluid viscosity and the applied normal force. At high rotational velocities in the 'hydrodynamic lubrication' regime the surfaces are pushed apart by lubrication forces and the measured sliding friction is dominated by the fluid rheology and thus becoming a function of the sliding velocity.

For such tribological measurements an apparent advantage of parallel plates in contrast to regular tribological setups as pin-on disk or ball-on three-plate fixtures is the knowledge of the surface area A over which the surfaces are in contact and a well defined flow field in-between. However, in particular for very flat surfaces even a small misalignment angle α between the plates leads to a localized contact of the surfaces and thus an ill-defined contact area that also varies over a full rotation of the plates. The triborheometrical setup introduced by Kavehpour et al. (Kavehpour and McKinley 2004) allowed to reduce the plate misalignment α with regard to non-parallelism. They employed a method of parallel alignment by bringing the movable surfaces into direct contact and a subsequent fixation of this position and parallel alignment. However, this alignment method still maintains the inherent non-perpendicularity of the plate geometry to the rotational axis.

For theoretical considerations of this flow problem of non-perpendicular parallel plates it is often assumed that only one plate carries this perpendicularity error and rotates against a perfectly aligned second surface, as this assumption leads to a steady flow over a rotation of the surface that is easier to model (Andablo-Reyes, Hidalgo-Alvarez et al. 2010; Andablo-Reyes, de Vicente et al. 2011; Andablo-Reyes, Hidalgo-Alvarez et al. 2011; Clasen 2013). In reality the perpendicularity error is maintained for both surfaces and leads to an oscillating gap distance that changes during one plate rotation between a parallel alignment of the surfaces and the maximum misalignment of 2α.

In the boundary lubrication regime the effect of this oscillation on the measured torque is substantial. The best experimental approach to deal with this problem in the boundary lubrication regime was so far to measure at least over one rotation cycle and to determine and report an average torque (Kavehpour and McKinley 2004). But then the question arises in how far this average value can represent the true boundary lubrication for a given sliding velocity. In this case not only the contact area but also the average gap changes during the rotation. Furthermore, the requirement of at least a full rotation cycle limits the use of this technique for low sliding velocities due to the required long measuring times.

In the hydrodynamic lubrication regime of a tribological measurement at high angular velocities the gap between the plates increases due to strong lubrication forces. The oscillations in the measured torque are therefore decreasing due to the diminishing gap-error to gap ratio and can regularly be neglected.

However, it has been shown that this remaining non-parallelism will lead to an extra hydrodynamic lubrication flow between the two surfaces (Clasen 2013). The magnitude of this extra lubrication flow does not depend on the surface properties or roughness of the two surfaces, but solely on the geometrical parameters of the surfaces, in particular the perpendicular misalignment angle and the flatness. In case that these geometrical parameters are known this hydrodynamic lubrication regime can be used to evaluate the high shear viscosity (Clasen 2013). However, this extra hydrodynamic lubrication due to non-parallelism does not represent the 'true' hydrodynamic lubrication in the sense of a tribological experiment that originates rather from the structure and interaction of the surface material with the fluid.

In order to account for the problems that arise for both high shear rheometry and tribology from fixed parallel plates due to non-parallelism and non-perpendicularity in this paper a novel measurement device is presented. This device allows a continuous self-aligning of the shearing surfaces during rotation. This is achieved via a low friction single contact point bearing on which the lower shearing surface is resting. This contact point is in line with the rotational axis of the rotating shearing surface, and in plane with the surface of the static shearing surface that can now ideally force-free adjust its tilt angle towards the other surface and approach true parallelism. In addition to the experimental setup first results on model Newtonian fluids are presented. The paper evaluates in particular the errors and limits for rheological measurements in a controlled gap mode for high shear rate experiments that are not accessible with a regular "fixed" parallel plate geometry. Furthermore the limits of applicable normal forces and sliding velocity in comparison to triborheometrical experiments with misaligned plates are determined.

Experiments and Methods

The SAPP fixture

The self-aligning parallel plate (SAPP) fixture is shown as a schematic drawing in Fig. 1.

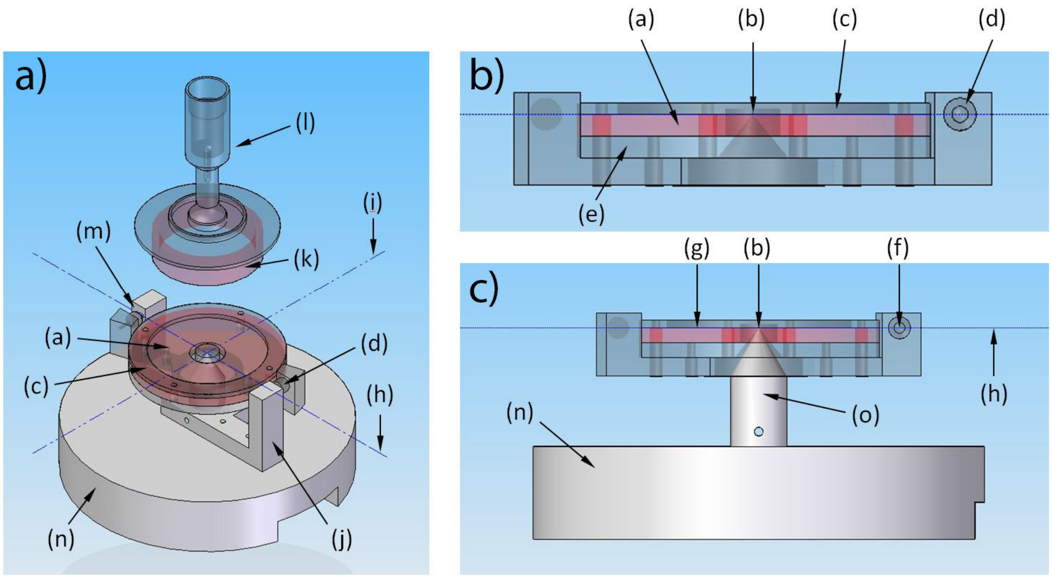

Fig. 1 Schematic drawing of the self-aligning parallel plate (SAPP) assembly with a) the angled view of the full assembly; b) side view of the lower shearing surface assembly; c) side view of the lower shearing surface assembly plus the conical tip on which the assembly is resting. Detailed description of parts: (a) exchangeable lower ring-shaped shearing surface; (b) contact point of the lower shearing surface assembly; (c) clamping ring and counterweight, holding the lower shearing surface in place; (d) ball bearing; (e) holding plate for the lower shear surface; (f) tip of the ball bearing; (g) surface of the lower ring-shaped shearing surface; (h) tilt axis 1 of the lower shearing surface assembly; (i) tilt axis 2; (j) static holder restricting the rotation of the lower shearing surface assembly; (k) exchangeable upper shear ring; (l) holder of the upper shear ring and connection to the rotational axis of the rheometer; (m) resting surface of the static holder against the ball bearing tip; (n) adjustable clamp to fix the assembly to the rheometer peltier element; (o) pin with conical tip of hardened steel, carrying the lower shearing surface assembly.

The lower shearing surface assembly (shown in Fig. 1b) is resting on a conical tip of hardened steel (o) that is fixed via a clamp (n) perpendicular to the Peltier unit of the rheometer. This tip can be centered towards the rotational axis of the device with four setscrews in the clamp. The holding plate (e) of the lower shearing surface is resting on this single contact point (b) as shown in Fig. 1c and can freely tilt around this point. The exchangeable lower shear ring (a) is clamped to the holding plate (e) with the clamping ring (c) such that the plane of the lower shearing surface (g) is in plane with the contact point (b). While the lower shearing surface assembly can freely tilt around the contact point (or the two tilt axis (h) and (i)), it cannot rotate around the rotational axis of the rheometer. This rotation is hindered by the static holder (j) against whose surface (m) two precision ball bearings rest that are held by two arms of the lower shearing surface assembly (see Fig. 1a, it should be noted that the design of the static holder allows only a clockwise rotation of the upper shearing surface). Since the tips (f) of the ball bearings are also in plane with the shearing surface (g) and in line with the tilt axis (h) the lower shearing assembly can still freely tilt around the axis (h) (only limited by the friction of the point contacts at (b) and (f)). Furthermore, the tilting around the other axis (i) is also still freely possible as the ball bearings allow movement of their tip contact points (f) along the resting surface (m). This tilting is thus only limited by the rolling friction of the precision ball bearings. In order to minimize gravitational effects on the free tilting of the lower shearing surface assembly, its center of gravity can be adjusted to lie in the contact point (b) by adjusting the mass of the clamping ring (c). This adjustment can be necessary to exactly counterweight the mass of the different exchangeable shearing surface rings for highly precise measurements at low rotational velocities and low applied normal loads.

The upper shearing surface assembly consists of the exchangeable upper shear ring (k) that is mounted via the standard exchangeable geometry connection tool of the rheometer to the upper rotational axis (l). The dimensions of the shearing surface area are for the current setup $R_1 = 20.37$ mm and $R_2 = 22.62$ mm where R_1 and R_2 are inner and outer radius of the thin ring-shaped area. It should be noted that the upper shearing surface is carrying forward the slight misalignment of the upper connection tool of the rheometer that is inherent to even the most precise instruments on the market. However, the purpose of the freely tilting lower surface is to self-align parallel to the upper (misaligned) surface. When operating the device in a tribological mode with an applied normal load F_N the alignment of the surfaces due to direct contact is evident. Operating in a controlled gap mode the alignment is caused by the hydrodynamic lubrication force F that arise during the rotation of the upper against the static lower shearing surface with an angular velocity Ω. The total hydrodynamic lubrication force caused for the thin ring-shaped surfaces by the misalignment angle α between the surfaces is (Clasen 2013)

$$F = \frac{\eta \Omega \sin \alpha}{h^3} \frac{A^3}{8\pi \bar{R}} \tag{1}$$

where η is the viscosity of the medium in the gap, h is the minimum gap distance between the surfaces, $A = \pi\left(R_2 - R_1\right)$ is the shearing surface area and $\bar{R} = \left(R_2 + R_1\right)/2$ is the average radius. The normal force arising due to the misalignment of the surfaces is highest at the lowest surface separation and thus driving the (tilting) lower plate back into parallelism. As it can be seen from eq. (1) this aligning force is proportional to Ω and thus working only at high enough angular velocities. However, the normal force is also proportional to h^{-3} and therefore increasingly effective when lowering the gap towards micrometer separations. Furthermore, the possibility to move the center of mass of the tilting plate to the contact point (b) via adjustment of the mass of (c) minimizes the gravitational force against which the lubrication force needs to act. Also for tribological experiments where a gap separation on the micrometer level is caused by the hydrodynamic lubrication flows the aligning normal forces become highly effective to align the surfaces parallel.

It should be noted that Xie et al. (Xie, Zou et al. 2008) used a similar idea of self-aligning of tilting parallel disks via hydrodynamic lubrication to determine the pressure drop observed for the radial flow between the two disks in order to determine the high shear viscosity, but limited their investigation to gap separations > 50 μm. Similarly, Gong and coworkers introduced the idea to operate the parallel plate geometry of a rotational rheometer with the addition of elastic hydrogel surfaces in a tribological mode. Lubrication flows and the arising normal forces deformed the elastic surfaces and leveled out their misalignment (Gong, Kagata et al. 1999; Kagata, Gong et al. 2002; Kagata, Gong et al. 2003). And recently McKinley and coworkers introduced for tribological measurements a spring mount that replaces the fixed connection of a shearing surface to the rotational axis of a rheometer with a degree of flexibility that also allows a shearing surface to align towards a second surface upon direct contact (Medina, Aadil et al. 2011).

The upper shear and lower shear rings (a) and (k) in Fig. 1a are exchangeable in order to allow the testing of different surface materials in tribological experiments. For the current investigation the lower plate is made from stainless steel and the upper plate from aluminum. It should be noted that in principle the shearing surfaces should be as flat as possible in order to avoid additional lubrication flows. However, for the current investigation no special attention has been paid to improve the flatness of the surfaces and they have been used as provided from the milling process of the manufacturer.

Shear stresses σ_{21} are calculated from the measured torque T for the thin ring shaped surface via (Kavehpour and McKinley 2004)

$$\sigma_{21} = \frac{2\bar{R}}{R_2^4 - R_1^4} T \qquad (2)$$

The rheometers onto which the SAPP fixture was mounted in this study were an AR 2000 and an AR-G2 from TA Instruments. However, it should be noted that the SAPP fixture can easily be mounted on any single head rheometer.

For general rheological measurements a cone-and plate fixture with a diameter of 4 cm and a 1° cone angle was used.

Fluid samples

The investigated test fluids were polydimethyl siloxane PDMS melts of nominal viscosities of 350 mPa s (Rhodorsil silicone oil 47V350) and of 5 Pa s (Rhodorsil silicone oil 47V5000) supplied by VWR Int. SAS (Briare, France).

Measurements procedure

All experiments with the new fixture presented in the following are conducted in an overfilled condition. The exposed shearing surface of (a) within the clamping ring (c) is covered with a millimeter thin layer of the test fluid and the upper shear ring (k) is subsequently immersed into this fluid to the desired gap height.

The zero-gap position between the tilting plates can be determined as an absolute value since the lower surface assembly will align upon direct contact parallel to the top surface for any rotational position of the top surface. The gap distance precision between the shearing surfaces that can be achieved in this way is on the order of micrometers, limited only by the positioning precision of the top plate via the rheometer. In Fig. 2 the results of a zero-gap determination procedure for the new fixture are shown. The position of the top surface is stepwise decreased and the eventual increase in normal force F_N is monitored by the rheometer. As it can be seen for dry surfaces (open symbols) upon contact the normal force gradually increases over a distance of 4 μm before a linear increase of F_N with decreasing gap is observed. This gradual increase is due to a sliding friction between the nearly parallel surfaces that initially hinders the final parallel alignment of the tilting plate and shows up as an apparent normal force even before the surfaces are in full contact. The addition of a lubricant (as for example the sample itself) diminishes this friction and leads to a sharp upturn of the normal force upon contact of the plates (closed symbols in Fig. 2) and a precise determination of the contact position. The lubricant increases, however, the time required for the normal force to reach a steady state due to the slower relaxation of the fluid via a squeeze flow.

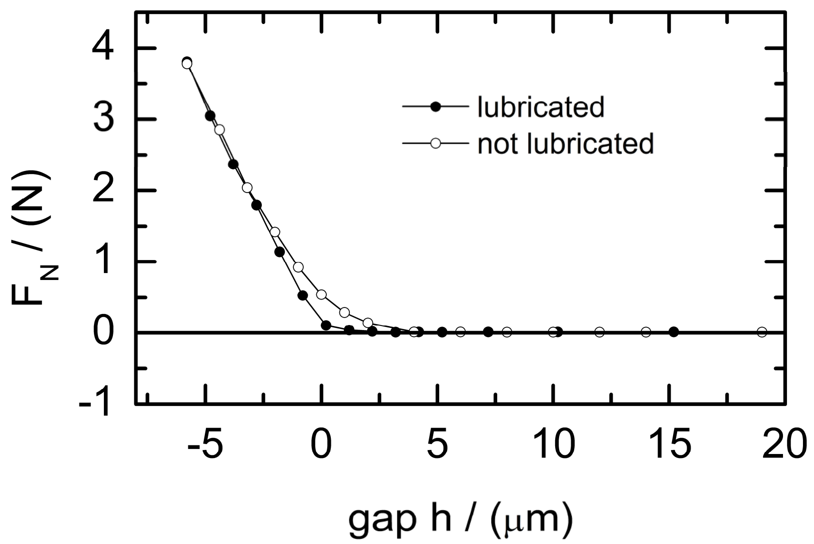

Fig. 2 Determination of the absolute zero-gap position by step-wise decreasing the position of the rheometer head and monitoring the normal force. Open symbols indicate results for a 'dry' determination, closed symbols are obtained using the sample oil (390 mPa s PDMS) as a lubricant between the surfaces.

Results and Discussion

The SAPP in a controlled gap mode

In a first instance the novel self-aligning fixture can be used as a regular rheometer. With the possibility to determine an absolute zero gap position with micrometer precision as demonstrated in Fig. 2, the self-aligning of the plates allows to access controlled micrometer gap distances for steady shear flow experiments. The accessible shear rate range of the tilting plates operated at a constant gap will indirectly be influenced by the misalignment of the top shearing surface and the inertia of the lower assembly. At low rates a limit arises due to the hydrodynamic lubrication forces necessary to align the surfaces parallel. If the rates are too low to create enough lubrication forces to work against the inertia of the lower plate in order to move it to maintain parallelism, the apparent measured stress will become larger (in particular if the center of gravity of the lower assembly is not coinciding with the contact point). Similarly, at too high rotational velocities of the upper plate the lubrication forces may not be large enough to accelerate the necessary tilting of the lower assembly fast enough to maintain parallelism. These limits will be explored in the following.

Figure 3 gives the apparent flow and viscosity curves for the PDMS oil with a nominal zero-shear viscosity of 390 mPa s, obtained with several gap settings spanning a range from 95 to 3 μm. For comparison also the bulk data obtained with a cone-and-plate geometry are shown. For the self aligning fixture data are only given down to shear rates where reliable steady state values could be achieved. As it can be seen, for the largest gap of 95 μm shear rates of at least 300 s^{-1} are necessary in order to have lubrication forces sufficiently aligning the plates. It should, however, be noted that for the current setup the mass of the clamping ring (c) in Fig. 1 is not adjusted so that the center of gravity of the fixture is below the tilt point (b). As discussed above, raising the center of gravity into the tilt point will diminish the forces required for tilting the plate and thus lower the required angular velocities or shear rates to align the surfaces.

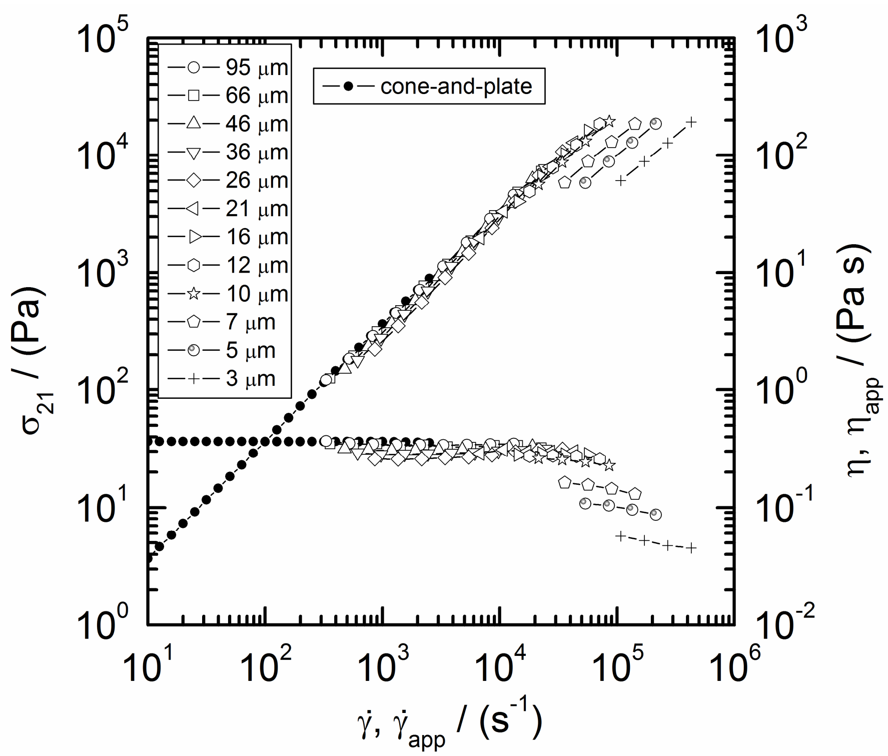

Fig. 3 Shear stresses σ_{21} and apparent viscosities η_{app} for the PDMS oil of nominal viscosity 390 mPa s as a function of the apparent shear rate $\dot{\gamma}_{app}$, determined at different gap settings (open symbols). For comparison the bulk data as function of the actual shear rate $\dot{\gamma}$ obtained with a cone-and-plate geometry are given as closed symbols.

The general upper limit for the shear rates was given by a maximum angular velocity that could be achieved. For the current setup above an angular velocity of 40 rad/s the tilting plate began to show visible vibrations which went along with a sudden increase in the measured torque. These vibrations occurred independent of the gap setting and are likely driven by the inertia of the tilting plate in combination with the non-perpendicularity of the upper plate to the rotational axis.

With decreasing gap the flow and viscosity curves start to deviate from the bulk viscosity data. This is not unexpected, as both wall slip and the remaining gap error due to non-flatness of the shearing surface are going to show up at these small gap settings. A possible slip is analyzed following the Mooney method (Mooney 1931; Cohen and Metzner 1985; Yoshimura and Prudhomme 1988) by plotting the apparent shear rate as a function of the inverse gap

$$\dot{\gamma}_{app} = \dot{\gamma} + \frac{2v_s}{h} \quad . \tag{3}$$

From the slope which represents the total slip velocity $2v_s$, one can calculate the extrapolation length $\varepsilon_{slip} = 2v_s/\dot{\gamma}$. In Fig. 4a such apparent shear rates are plotted vs $1/h$ for five different constant stress levels (closed symbols), and the resulting extrapolation lengths ε_{slip} as well as the resulting viscosities $\eta = \sigma_{21}/\dot{\gamma}$ obtained from the extrapolated true bulk shear rates are plotted (also as closed symbols) with their uncertainties in Fig. 4c.

Similarly the general determination of a misalignment error ε in a parallel plate configuration is done via an extrapolation of apparent viscosity measurements at varying gaps h (Kramer, Uhl et al. 1987)

$$\frac{1}{\eta_{app}} = \frac{1}{\eta} + \frac{\varepsilon}{h}\frac{1}{\eta} \quad . \tag{4}$$

It can easily be shown that the two equations are actually probing the same error and that $\varepsilon_{slip} = \varepsilon$. Figure 4b shows (as open symbols) also a misalignment error analysis by plotting the inverse apparent viscosities of Fig. 3 for different gaps at two constant shear rates. The obtained true viscosities η and the misalignment error ε are also plotted in Fig. 4c (open symbols). As expected both the extrapolation length ε_{slip} and the error ε show similar values. Figure 4c indicates, however, that only at higher shear rates the error approaches a constant value of ~ 3.4 µm. At lower rates lubrication forces are not sufficiently strong to align the interfaces and the alignment error increases with decreasing shear rates.

Although it is in principle not possible to separate the contributions of slip and misalignment to the determined value of $\varepsilon \sim$ 3.4 µm, it can be argued that slip of a homogeneous polymer melt is expected to occur over much smaller length scales (Granick, Zhu et al. 2003). The main contribution to ε would then be the misalignment, and since the self-aligning of the surfaces diminishes effects of non-parallelism, the remaining gap error of 3.4 µm will mainly be caused by the non-flatness of the shearing surfaces.

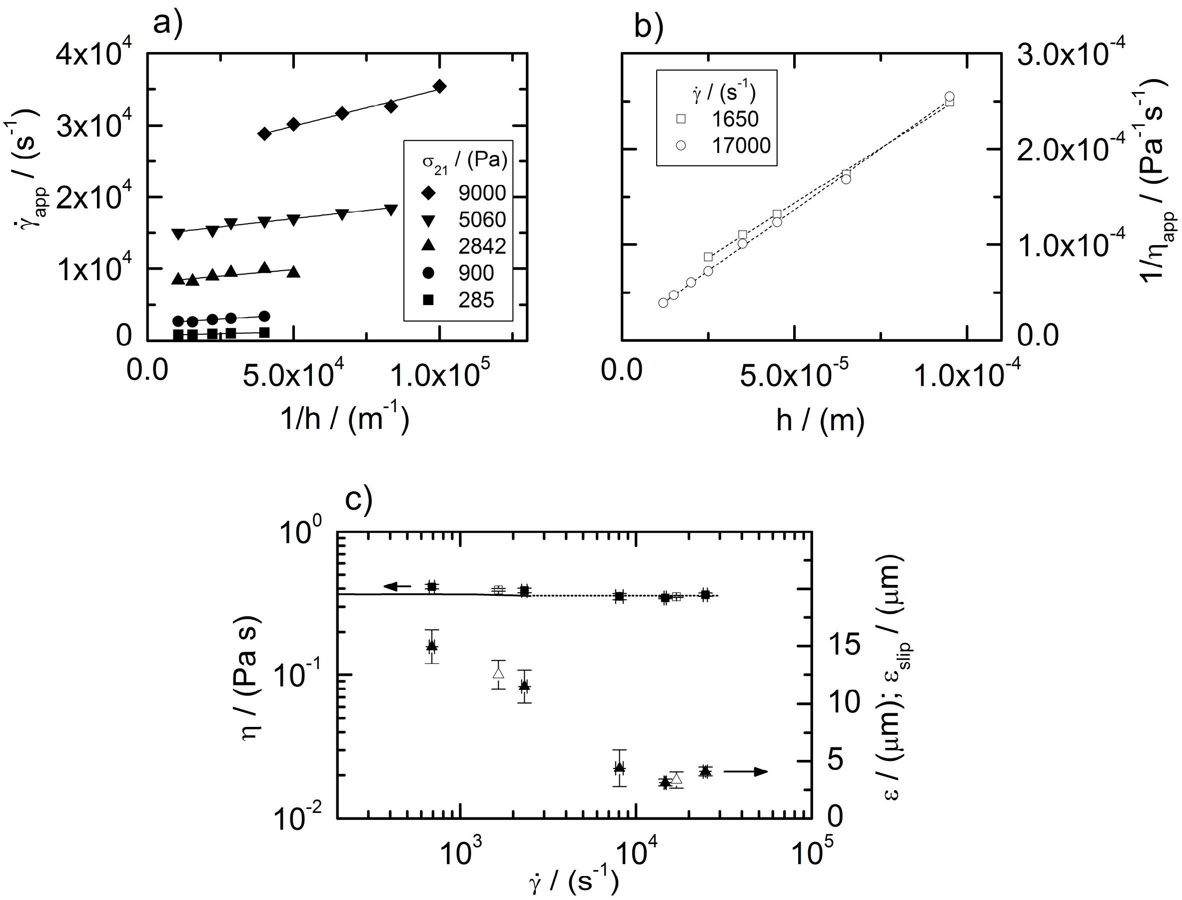

Fig. 4 Analysis of slip and/or misalignment errors of the data of Fig. 3. a) Mooney analysis following eq. (3), apparent shear rates plotted as a function of the inverse gap for constant stress levels as indicated in the legend (closed symbols). Solid lines are fits to eq. (3). b) Misalignment analysis, open symbols are inverse apparent viscosities plotted as function of the gap h, and dotted lines are fits to eq. (4) to determine the misalignment error. c) True viscosities η as a function of the actual shear rate $\dot{\gamma}$ resulting from the fits of eq. (3) (closed squares) and fits of eq. (4) (open squares) in Fig. 4a. Furthermore the resulting extrapolation length ε_{slip} (closed triangles) and misalignment error ε (open triangles) are given.

The SAPP in a tribological mode

The second objective for designing the SAPP fixture was to minimize errors arising from non-parallelism for tribological measurements when utilizing a plate-plate type fixture in a rotational rheometer. As shown in (Clasen 2013), a major issue with using fixed parallel plates for tribological measurements was the uncontrolled misalignment angle that prevented an *a priori* determination and

control of the hydrodynamic lubrication. Even more difficult, however, was the evaluation of the boundary lubrication regime at low angular velocities for fixed plates with perpendicularity errors towards the rotational axis in both plates. This lead to a transition over a full rotation of the plates from a perfect alignment to a maximum misalignment of 2α and strong variations in the applicable normal load and the measurable shear force (Clasen 2013). The novel design of the SAPP fixture removes this misalignment towards the rotational axis and reduces misalignment errors over a full rotation to the non-flatness of the surfaces.
Figure 5 gives the results of experiments conducted with the new fixture in a tribological mode. The shear stress σ_{21} is plotted as a function of the angular velocity Ω under an applied normal load F_N with which the shearing surfaces are pushed together. The data is presented in form of so called Stribeck curves: friction factor $\mu = F_S/F_N = \sigma_{21}A/F_N$ as a function of the Gumbel number which is $\sim \Omega\bar{R}\eta/\left(F_N/\Delta R\right)$. Here ΔR represents the characteristic width over which the normal load F_N is applied. These dimensionless numbers are generally used for tribological experiments since they do not require knowledge of the often not defined surface area A or gap distances in tribological setups. For the ring shaped surface $\Delta R = R_2 - R_1$ and the Gumbel number is in this case conveniently defined as $Gu = \Omega\eta A/F_N$ with $A = \pi\left(R_2^2 - R_1^2\right)$ as the surface area of the ring. It is this Gumbel number against which the sliding friction is plotted in Fig. 5. It should also be noted that calculating the Gumbel number requires a viscosity for which in the following the zero-shear values of the PDMS oils are used.

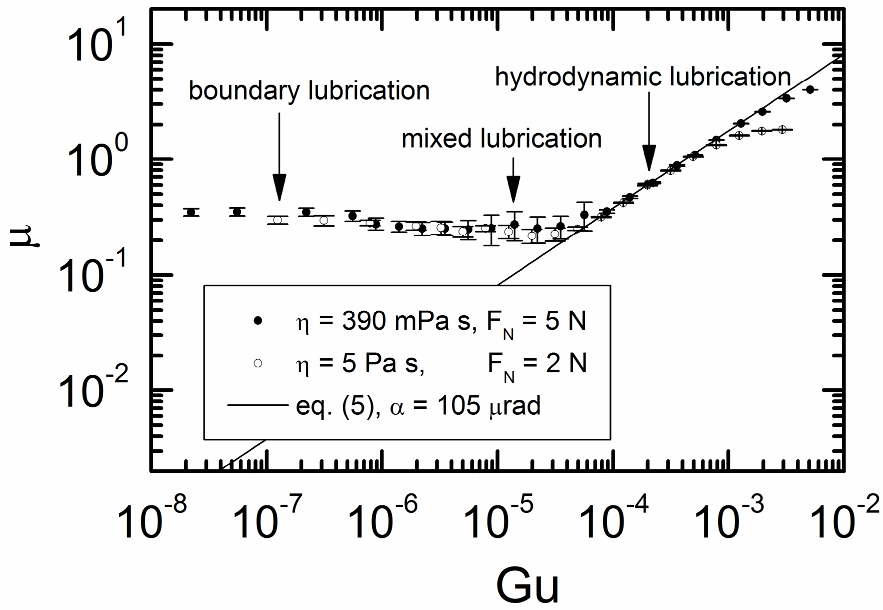

Fig. 5 Stribeck curves – sliding friction μ as a function of the Gumbel number *Gu*. The solid line is a least square fit of the theoretical hydrodynamic lubrication regime data with eq. (5).

For higher angular velocities or Gumbel numbers above $\sim 10^{-4}$ we observe a hydrodynamic lubrication regime for which a typical scaling of the friction factor with the Gumbel number of

$$\mu = C^{1/3} Gu^{2/3} \qquad (5)$$

is observed (Clasen 2013). The constant $C = K/\sin\alpha$ contains in addition to a geometrical parameter $K = \pi\left(R_1 + R_2\right)^2 / 2\left(R_1 - R_2\right)^2$ also the sine of the apparent misalignment α that causes the lubrication flow and the hydrodynamic lift. As it can be seen from Fig. 5, the hydrodynamic lubrication regime can well be fitted with eq. (5) and yields α = 105 μrad. Furthermore this α is independent of the fluid viscosity. The Stribeck curves of the two different fluids investigated with the same shearing surface combination coincide in Fig. 5 and thus yield the same misalignment angle. This angle is solely related to the non-flatness of the surfaces as the self-alignment of the surfaces removes the non-parallelism error that was present in previous studies (Andablo-Reyes, Hidalgo-Alvarez et al. 2010; Andablo-Reyes, de Vicente et al. 2011; Clasen 2013). A rough comparison to the gap error determined for the controlled gap experiment supports this hypothesis as $2R_2 \tan\alpha =$ 4.75 μm, which is of the same order of magnitude as the gap error $\varepsilon \sim$ 3.4 μm. This misalignment could be further reduced by improving the

flatness of the surfaces of the shear rings. In the present study we have, however, deliberately used the shearing rings with their surfaces as they were obtained from a regular milling procedure in order to assess the amount of error expected for the new fixture.
An upper limit for the Gumbel number was in both cases reached around Gu = 0.003. For the lower viscosity sample this was again determined by a critical angular velocity above which the fixture exhibited visible vibrations. However, compared to the controlled gap experiments this limit was reached for tribological experiments at a higher angular velocity of 100 rad/s. For the higher viscosity sample an upper angular velocity limit was reached at 10 rad/s. Above this velocity the measured torque showed strong fluctuations and did not reach a steady state. The reason for these fluctuations still needs to be investigated.
It should be noted that the deviation from the 2/3 scaling of eq. (5) observed for both samples at high Gumbel numbers in Fig. 5 are not related to the above mentioned experimental limitations. Although considered Newtonian both samples actually exhibit an onset of shear thinning at higher rates that also leads to a lowering of friction factors. Furthermore, for the higher viscosity sample the normal stresses of the fluid eventually reach the same order of magnitude as the applied normal load. This leads to a limiting plateau of the friction factor that is depending on this applied normal load (Clasen 2013).

The tribological data in Fig. 5 give also the standard deviation of the stress signal over at least one full rotation in order to judge the maximum error achievable. It can be seen that the intermediate regime has a relatively large error. In this so-called ‘mixed lubrication’ regime only a partial onset of hydrodynamic lubrication is attained and the randomly occurring direct interaction of the surface asperities are causing the torque signal to fluctuate. As the Gumbel number is increased and the full hydrodynamic lubrication regime is reached the error becomes small. In the hydrodynamic lubrication regime the lubrication forces push the shearing plates apart and the surface asperities are not in contact anymore so that the fluctuation in the torque is minimized. However, it is in particular the boundary lubrication regime at small Gumbel numbers where the new SAPP fixture demonstrates the strength of the self-aligning of the plates. For fixed plate positions in this regime strong fluctuations of the torques over a single rotation are observed and prohibited inherently a quantitative evaluation of the boundary lubrication (Clasen 2013). With the self-aligning plates these fluctuations are strongly reduced and well below those of the mixed lubrication regime as the error bars in Fig. 5 indicate. It is therefore possible to compare now the lubricating properties of the two samples in the boundary lubrication regime. As it can be seen, the rate independent sliding friction μ is for the two PDMS oils also independent of the viscosity level or the applied normal load, as expected for fluids of similar chemical composition.

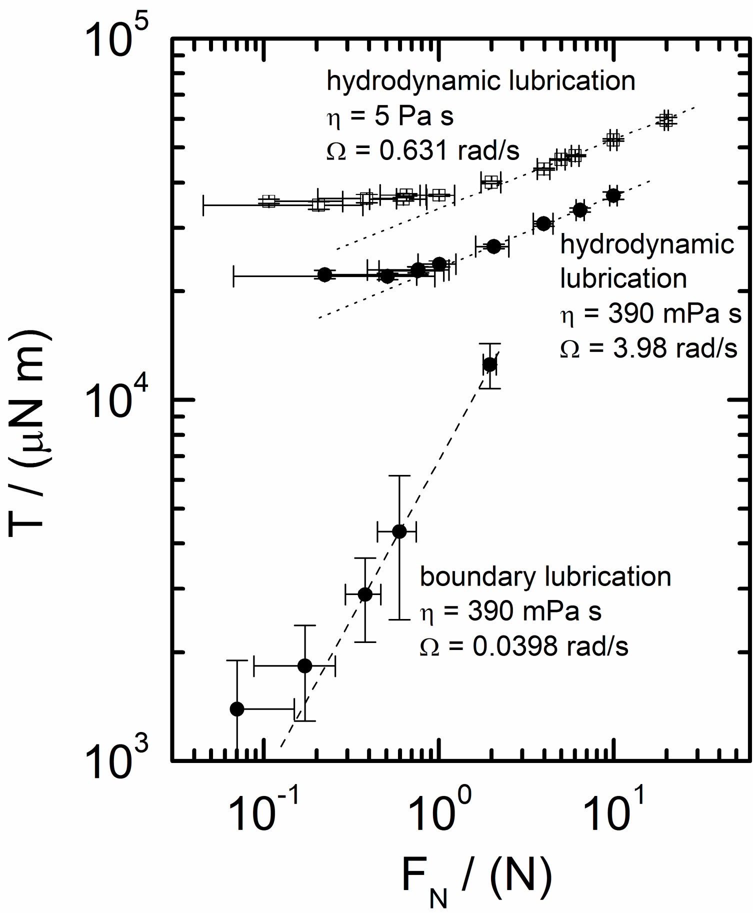

Fig. 6 Average values of the torque T over at least one full rotation of the shearing surfaces as a function of the applied normal load F_N for series of constant rotational velocities.

To further explore the capabilities of the SAPP fixture, Fig. 6 shows results for tribological measurements at constant angular velocities Ω, but varying normal loads F_N. Generally one requires a minimum amount of normal load to ensure a sufficient interaction of the surfaces. The angular velocities have been chosen to probe either the boundary lubrication or the hydrodynamic lubrication regime. In the boundary lubrication regime one expects a linear relation of the torque T to the normal load as the friction factors are constant. As it can be seen in Fig. 6 this linear relation (dashed line) is followed down to normal loads of 0.4 N, but below this limit the torque is deviating towards higher values. Similarly, for the hydrodynamic lubrication regime one expects a power law dependence of the torque on the normal load following eq. (5). For the logarithmic presentation of the data in Fig. 6 it can be seen that the expected constant slopes calculated from eq. (5) (dotted lines) are followed down to normal loads of 2N, validating thus the normal loads applied for obtaining the Stribeck curves in Fig. 5. For normal loads below this limit, the torque exhibits systematic deviations towards higher values. It should be noted that this systematic deviation cannot be inferred from the observed error in the torque signal over a full rotation (error bars in Fig. 6), which is much smaller than the observed deviations. In contrast to this the observed error on the applied normal force in Fig. 6 is directly related to the experimental settings and can be linked to the tolerance window of the applied normal force. For the current experiments the rotational rheometer controlled the normal forces within 0.3 N, which had proven to be a practical limit for the tribological experiments. For requested normal loads below 0.6 N the tolerance was reduced to 0.1 N which represented the lower limit of the rheometer capability for the tolerance as well as for the applicable normal force. It should be noted that these lower limits of the applicable normal force of 0.4 N for the boundary lubrication and 2 N for the hydrodynamic lubrication regime correspond for the current shearing surface area to low minimum pressures of 1.3 and 6.5 kPa respectively.

Comparison of the controlled gap and the tribological mode

One can now compare the two different modes and regular rotational rheometry with regard to their capability to measure viscosities at high shear rates. Correcting the gaps of the controlled gap measurements of Fig. 3 with the gap error ε = 3.4 µm from Fig. 4c allows calculating the actual viscosities over the shear rate range for which a constant gap error is observed. These results are given in Fig. 7 for the different investigated gap settings. It can be observed in Fig. 7 that for gap settings down to 10 µm (small closed symbols) the viscosities show excellent agreement with an extrapolation of the bulk viscosity data (dashed line) obtained with a regular cone and plate geometry. However, it can also be observed that for gaps below 10 μm (small open symbols) the viscosities exhibit a sudden decrease even when taking into account the misalignment error. This gap of 10 μm represents therefore the lower limit for applying the novel fixture in a controlled gap mode. Below this limit the gap error due to non-flatness of the surfaces is directly affecting the measurements.

For the tribological measurements we can now use the determined angle α to obtain the high shear rate viscosity curves from the hydrodynamic lubrication regime data. As shown in (Clasen 2013) in this regime the viscosity and the shear rate are both related to the measured stress at a certain angular velocity via

$$\eta = \frac{\sigma_{21}^{\frac{3}{2}}}{\Omega} \sqrt{\frac{A}{CF_N}} \,. \tag{6}$$

and

$$\dot{\gamma} = \frac{\Omega}{\sigma_{21}^{\frac{1}{2}}} \sqrt{\frac{CF_N}{A}} \,. \tag{7}$$

The flow curves obtained from the tribological data via eqs. (6) and (7) are given in Fig. 7 (large open circles). They show excellent agreement with the controlled gap experiments. For the 5 Pa s sample the data is also compared with high shear rata data of the same fluid obtained with a FMR thin film rheometer (solid line, data taken from (Clasen, Kavehpour et al. 2010)).

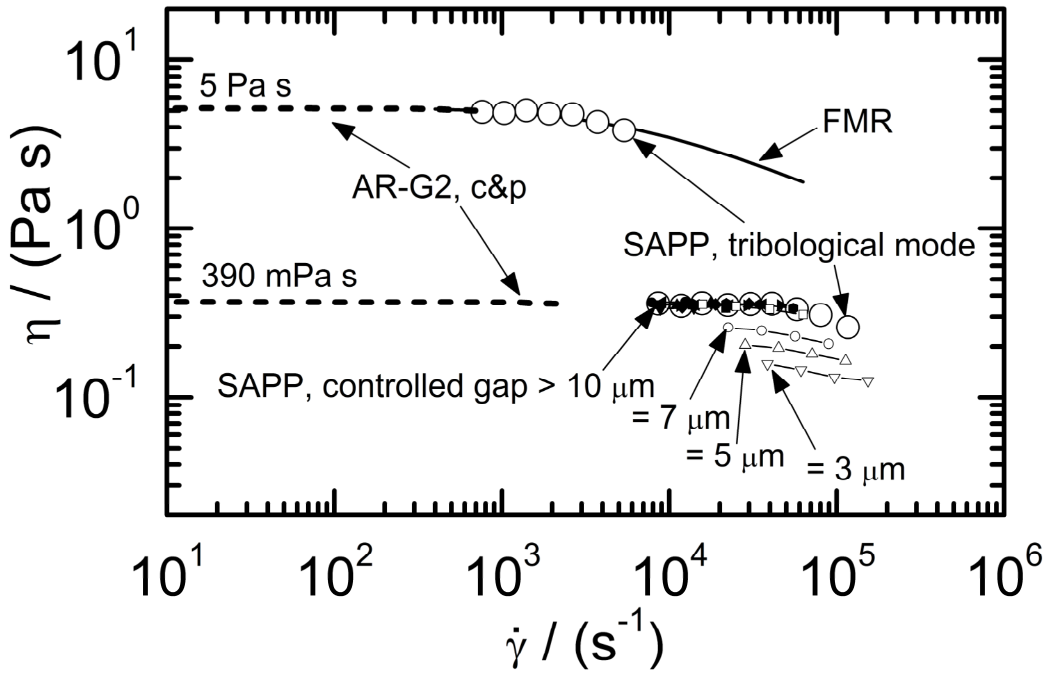

Fig. 7 Comparison of the viscosity curves obtained with the different devices. Dashed lines are bulk viscosities obtained with a cone-and-plate geometry of a regular rotational rheometer. Large open circles are viscosities calculated from the hydrodynamic lubrication regime of the tribological experiments of Fig. 5 with eqs. (6) and (7). Small closed symbols give the slip/misalignment corrected viscosities obtained with the SAPP at controlled gaps above 10 μm. Small open symbols give apparent slip/misalignment corrected viscosities from the SAPP fixture for gaps below 10 μm as indicated. The solid line gives for comparison high shear rate data obtained with a sliding plate rheometer for the 5 Pa s PDMS sample from (Clasen, Kavehpour et al. 2010).

Conclusion

In this paper we present a new self-aligning parallel plate fixture that can be mounted onto a single head rotational rheometer. This fixture uses hydrodynamic lubrication forces to continuously align a freely tilting plate towards a rotating shearing surface. The tilting of the plate occurs around a single contact point within the shearing surface while a rotation of the surface is hindered by a set of ball bearings resting with their contact points also within the shearing plane against the fixed outer frame of the fixture. The low frictional resistance in the point joint as well as the ball bearing against tilting motions of the plate lowers

the accessible angular velocities and measurable fluid viscosities in a controlled gap mode and reduces the required normal load for tribological experiments.
The experimental range of the new fixture has been evaluated with two PDMS melts of zero-shear viscosities of 350 mPa s and 5 Pa s. In a controlled gap mode it could be shown that the self-aligning of the fixture reduced the gap error to the flatness of the untreated shearing surfaces of $\varepsilon = 3.4$ µm. With this so far unmatched small gap error it was possible to obtain reliable flow curves from gap settings down to 10 µm with shear rates up to 10^5 s^{-1}.
In a tribological mode with an applied normal load the self-aligning of the plates reduced the friction coefficient error in the boundary lubrication regime over a full rotation well below 10 %. This enabled a quantitative comparison of the boundary lubrication of the sample liquids down to Gumbel numbers of $Gu = 10^{-8}$ or angular velocities of $\Omega = 398$ µrad/s. It could be shown that the friction coefficient in the hydrodynamic lubrication regime is determined by the misalignment caused by the non-flatness of the surface. The determination of this misalignment angle of $\alpha = 105$ µrad for the surface material used in this study enabled to access the viscosity of the test fluids. The flow curves that could be measured from the hydrodynamic lubrication flows reached similarly high shear rates as in the controlled gap mode of up to 10^5 s^{-1}.

Acknowledgement

The author would like to acknowledge financial support from the FWO-Vlaanderen (project G.0543.10N) . Furthermore Dr. S.J. Baik is acknowledged for fruitful discussions on the design of the first version of this fixture.

References

Andablo-Reyes, E., J. de Vicente, et al. (2011). "On the nonparallelism effect in thin film plate-plate rheometry." Journal of Rheology **55**(5): 981-986.
Andablo-Reyes, E., R. Hidalgo-Alvarez, et al. (2010). "A method for the estimation of the film thickness and plate tilt angle in thin film misaligned plate-plate rheometry." Journal of Non-Newtonian Fluid Mechanics **165**(19-20): 1419-1421.
Andablo-Reyes, E., R. Hidalgo-Alvarez, et al. (2011). "Controlling friction using magnetic nanofluids." Soft Matter **7**(3): 880-883.
Baik, S. J., P. Moldenaers, et al. (2008). Determination of normal stresses in micrometer thin films. Xvth International Congress on Rheology - the Society of Rheology 80th Annual Meeting, Pts 1 and 2. A. Co, L. G. Leal,

R. H. Colby and A. J. Giacomin. Melville, Amer Inst Physics. **1027:** 1165-1167.
Baik, S. J., P. Moldenaers, et al. (2011). "A sliding plate microgap rheometer for the simultaneous measurement of shear stress and first normal stress difference." Review of Scientific Instruments **82**(3): 035121.
Barnes, H. A. (2002). Viscosity. Aberystwyth, The University of Wales Institute of Non-Newtonian Fluid Mechanics.
Chevalier, J. and F. Ayela (2008). "Microfluidic on chip viscometers." Review of Scientific Instruments **79**(7): 3.
Clasen, C. (2012). "Determining the true slip of a yield stress material with a sliding plate rheometer." Rheologica Acta **51**(10): 883-890.
Clasen, C. (2013). "High shear rheometry using hydrodynamic lubrication flows." Journal of Rheology **57**(1): 197-221.
Clasen, C., B. P. Gearing, et al. (2006). "The flexure-based microgap rheometer (FMR)." Journal of Rheology **50**(6): 883-905.
Clasen, C., H. P. Kavehpour, et al. (2010). "Bridging Tribology And Microrheology Of Thin Films." Applied Rheology **20**(4): 196-208.
Clasen, C. and G. H. McKinley (2004). "Gap-dependent microrheometry of complex liquids." Journal of Non-Newtonian Fluid Mechanics **124**(1-3): 1-10.
Cohen, Y. and A. B. Metzner (1985). "Apparent Slip-Flow of Polymer-Solutions." Journal of Rheology **29**(1): 67-102.
Connelly, R. W. and J. Greener (1985). "High-Shear Viscometry with a Rotational Parallel-Disk Device." Journal of Rheology **29**(2): 209-226.
Crawford, N. C., S. K. R. Williams, et al. (2012). "Shear thickening of chemical mechanical polishing slurries under high shear." Rheologica Acta **51**(7): 637-647.
Davies, G. A. and J. R. Stokes (2008). "Thin film and high shear rheology of multiphase complex fluids." Journal of Non-Newtonian Fluid Mechanics **148**(1-3): 73-87.
Dontula, P., C. W. Macosko, et al. (1999). "Does the viscosity of glycerin fall at high shear rates?" Industrial & Engineering Chemistry Research **38**(4): 1729-1735.
Duda, J. L., E. E. Klaus, et al. (1988). "Capillary Viscometry Study of Non-Newtonian Fluids - Influence of Viscous Heating." Industrial & Engineering Chemistry Research **27**(2): 352-361.
Erickson, D., F. Z. Lu, et al. (2002). "An experimental investigation into the dimension-sensitive viscosity of polymer containing lubricant oils in microchannels." Experimental Thermal and Fluid Science **25**(8): 623-630.
Erni, P., M. Varagnat, et al. (2011). "Microrheometry of sub-nanolitre biopolymer samples: non-Newtonian flow phenomena of carnivorous plant mucilage." Soft Matter **7**(22): 10889-10898.
Gong, J. P., G. Kagata, et al. (1999). "Friction of gels. 4. Friction on charged gels." Journal of Physical Chemistry B **103**(29): 6007-6014.
Granick, S., Y. X. Zhu, et al. (2003). "Slippery questions about complex fluids flowing past solids." Nature Materials **2**(4): 221-227.
Henson, D. J. and M. E. Mackay (1995). "Effect of Gap on the Viscosity of Monodisperse Polystyrene Melts - Slip Effects." Journal of Rheology **39**(2): 359-373.

Kagata, G., J. P. Gong, et al. (2002). "Friction of gels. 6. Effects of sliding velocity and viscoelastic responses of the network." Journal of Physical Chemistry B **106**(18): 4596-4601.

Kagata, G., J. P. Gong, et al. (2003). "Friction of gels. 7. Observation of static friction between like-charged gels." Journal of Physical Chemistry B **107**(37): 10221-10225.

Kang, K., L. J. Lee, et al. (2005). "High shear microfluidics and its application in rheological measurement." Experiments in Fluids **38**(2): 222-232.

Kavehpour, H. P. and G. H. McKinley (2004). "Triborheometry from Gap-Dependent Rheology to Tribology." Tribology Letters **17**(2): 327-335.

Kelly, A. L., T. Gough, et al. (2009). "High Shear Strain Rate Rheometry of Polymer Melts." Journal of Applied Polymer Science **114**(2): 864-873.

Kojic, N., J. Bico, et al. (2006). "Ex vivo rheology of spider silk." Journal of Experimental Biology **209**(21): 4355-4362.

Kramer, J., J. T. Uhl, et al. (1987). "Measurement of the Viscosity of Guar Gum Solutions to 50,000 1/s Using a Parallel Plate Rheometer." Polymer Engineering and Science **27**(8): 598-602.

Kulicke, W. M. and R. S. Porter (1980). "High Shear Dependence of the Viscosity of Polymer Fluids." Journal of Rheology **24**(6): 890-891.

Medina, D. I., E. Aadil, et al. (2011). The development of an innovative triborheometry fixture/design to study the frictional dynamics of solid-liquid systems. The Society of Rheology 83rd Annual Meeting. Cleveland OH, USA.

Merrill, E. W. (1954). "A coaxial cylinder viscometer for the study of fluids under high velocity gradients." J. Coll. Sci. **9**: 7-19.

Mooney, M. (1931). "Explicit formulas for slip and fluidity." Journal of Rheology **2**: 210-222.

Mriziq, K. S., H. D. Cochran, et al. (2007). "Rheology and birefringence of Fomblin YR at very high shear rates." Rheologica Acta **46**(6): 839-845.

Mriziq, K. S., H. J. Dai, et al. (2004). "High-shear-rate optical rheometer." Review of Scientific Instruments **75**(6): 2171-2176.

Pipe, C. J., T. S. Majmudar, et al. (2008). "High shear rate viscometry." Rheologica Acta **47**(5-6): 621-642.

Tadmor, Z. and C. G. Gogos (2006). Principles of Polymer Processing. Hoboken, NJ, Wiley.

Xie, Z., Q. Zou, et al. (2008). "Design and verification of the pressure-driven radial flow microrheometer." Tribology Transactions **51**(4): 396-402.

Yoshimura, A. and R. K. Prudhomme (1988). "Wall Slip Corrections for Couette and Parallel Disk Viscometers." Journal of Rheology **32**(1): 53-67.